Published in final edited form as:
J Phys Chem Lett. 2010 ; 1(2): 544–549. doi:10.1021/jz900235f.

Emerging Methods for Producing Monodisperse Graphene Dispersions

Alexander A. Green and **Mark C. Hersam***
Department of Materials Science and Engineering and Department of Chemistry, Northwestern University, Evanston, Illinois 60208-3108, USA

Abstract

With the recent burst of activity surrounding solution phase production of graphene, comparatively little progress has been made towards the generation of graphene dispersions with tailored thickness, lateral area, and shape. The polydispersity of graphene dispersions, however, can lead to unpredictable or non-ideal behavior once they are incorporated into devices, since the properties of graphene vary as a function of its structural parameters. In this brief perspective, we overview the problem of graphene polydispersity, the production of graphene dispersions, and the methods under development to produce dispersions of monodisperse graphene.

Keywords

graphene; nanoribbon; separation; sorting; monodispersity; suspension; dispersion; solution

Introduction

Graphene, a honeycomb lattice of carbon only a single atom thick, has attracted considerable interest in the research community as a result of its outstanding properties. Sheets of graphene have demonstrated field effect mobilities in excess of 200,000 $cm^2/V\text{-}s$ [1] and exhibit quantum mechanical behavior[2]. Some researchers have proposed that future microprocessors could be fabricated by etching graphene wafers into desired device architectures[3], while closely packed graphene sheets could be employed in applications such as transparent conductors[4,5], field emission displays[6], and composite materials[7].

To date, many of the electrical and optical measurements of graphene have used samples produced by micromechanical cleavage in which small flakes of graphene are exfoliated by direct stamping or via an intermediary adhesive (i.e., "Scotch Tape")[8]. It is unlikely, however, that this method will be amenable to large scale production of graphene. Consequently, researchers are investigating a number of alternative means for producing graphene (see Ref. [9] for a review). Of these methods, solution phase techniques have shown great promise for industrial scale production of graphene and graphene nanoribbons (GNRs) (see Ref. [10] for a review). Despite this potential, most graphene dispersions contain large variations in the thickness, lateral area, and shape of the exfoliated graphene flakes. This polydispersity presents issues in many applications since the properties of graphene are inextricably linked to its structure. Research effort is thus shifting towards the development of methods for producing graphene with controlled structure, either by direct exfoliation into solution or through post-dispersion sorting techniques.

* m-hersam@northwestern.edu .

Structure-Property Relationships in Graphene

Graphene sheets consisting of fewer than ten layers possess electronic structure distinct from that of bulk graphite[3]. At such thicknesses, graphene properties vary as a function of layer number and interlayer ordering (Fig. 1A-B). Single-layer graphene, for instance, is a zero-gap semiconductor with a linear energy dispersion such that its charge carriers can be viewed as massless particles that travel at an effective speed of ~10^6 m s^{-1}. This unique band structure has made single-layer graphene a fascinating system for the study of quantum electrodynamics. Bilayer graphene is likewise a zero-gap semiconductor but its electrons obey a parabolic energy dispersion. Experiments have shown that a tunable band gap of several hundred meV can be induced in bilayer graphene by breaking the symmetry between the two graphene layers using a carefully applied gate bias[11]. These results suggest that bilayer graphene could be used for novel optoelectronic applications and future microprocessors. In contrast, trilayer graphene is a semimetal with a band overlap that can be controlled by an external electric field[12]. The above properties only hold for multilayer graphene with the Bernal ABAB stacking found in natural graphite. Deviations from this stacking arrangement, either through lateral translation or angular misorientation (Fig. 1B), can affect interlayer interactions and sometimes induce behavior similar to that of single-layer graphene[13].

The absence of permanent band gaps in graphene sheets makes their integration into conventional semiconductor device architectures difficult. As a result, direct band gap semiconducting GNRs with widths less than ~10 nm have also been proposed for graphene-based optoelectronics[14] (Fig. 1C). The production of graphene nanoribbons, however, brings with it a host of additional polydispersity and materials issues. Theoretical work has shown that the GNR band gap varies inversely with ribbon width and is further influenced by the ribbon edge type (e.g., zigzag vs. armchair)[14]. Furthermore, patterning of semiconducting GNRs from larger graphene sheets pushes the limits of conventional lithography, and defects introduced during the etching process can hinder device performance[15,16]. Accordingly, solution phase production coupled with post-dispersion separation may prove to be a superior pathway to GNRs with low defect density and reliable properties.

Dispersing Graphene in Solution

As a result of the strong van der Waals forces that bind graphene layers together, the exfoliation of pristine graphene into solution requires an energy input of over 2 eV per square nanometer of graphene surface[17]. Two main approaches have been utilized to overcome these forces: sonication of graphite in solvent systems and chemical functionalization or treatment of graphite to weaken interlayer interactions. Pristine graphite has been sonicated in organic solvents[18] and aqueous surfactant solutions[5,19] to yield graphene crystallites up to a few microns in lateral size. In this process, the cavitation of bubbles generated by ultrasonic fields produces shock waves that break apart the graphite flakes, which are subsequently stabilized by the solvent system. The most efficient solvents have surface energies close to that of graphene[18], which minimizes the energy cost associated with exfoliation. In addition, many of the common dispersants of carbon nanotubes have proven effective at dispersing graphene[5,19].

Several functionalized forms of graphite have been used to increase the yield and lateral extent of graphene exfoliated into solution. The most commonly used form is graphite oxide, a heavily functionalized derivative in which the edges and basal plane of the graphene are decorated with oxygen containing functional groups[20]. Single-layer graphene oxide (GO) sheets tens of microns in lateral size can be readily dispersed in water at concentrations higher than ~0.2 mg mL^{-1}. Despite its increased processability, graphene oxide is

electrically insulating and, even after chemical reduction, its electronic properties do not match those of pristine graphene[21]. To increase the graphite interlayer spacing and reduce interlayer attraction, it is also possible to add intercalants to the graphite flakes. In some cases, these intercalated flakes can be expanded by brief exposure to elevated temperatures. This thermal shock treatment causes volatile intercalants to rapidly escape from the graphite and results in a large increase in the spacing between graphene sheets perpendicular to the basal plane. These expanded and intercalated forms of graphite can then be exfoliated by sonication in solution[22,23].

The polydispersity of graphene dispersions can vary substantially depending on the method used to exfoliate them and the starting graphitic material. Sonication of naturally occurring graphite flakes in N-methylpyrrolidone accompanied by weak centrifugation results in a supernatant in which ~85% of the graphene is evenly distributed in thickness from one to three layers with the remainder being up to 13 layers thick[18]. Despite these large variations, graphene from such dispersions is relatively large at a few microns in lateral size and has low defect levels, which makes it promising for electronic applications. Other researchers[23] have shown that dispersions consisting of ~90% single-layer graphene can be generated by intercalating expanded graphite with oleum and tetrabutylammonium hydroxide followed by sonication in a phospholipid-polyethyleneglycol surfactant. The main drawback of this approach is the comparatively small size of the graphene sheets at ~250 nm mean lateral extent.

For GO, which is typically exfoliated as single-layer sheets, one of the main polydispersity challenges arises from variations in the lateral area of the flakes. It has been shown that the mean lateral size of GO can be shifted from 400 nm to 20 μm by changing the graphite starting material and the sonication conditions[24]. For a given set of processing conditions, however, the GO lateral size can vary by up to two orders of magnitude. Such variations in flake area can lead to inhomogeneous GO films, which limits performance in applications such as transparent conductors and supercapacitors.

In recent work, several groups have produced GNRs via direct exfoliation into solution or by longitudinally unzipping carbon nanotubes. Researchers have found that sub-10-nm wide GNRs with smooth edges can be produced by sonication of expanded graphite in 1,2-dichloroethane with the assistance of a conjugated polymer[22]. Later work utilized plasma etching to slice open carbon nanotubes embedded in a polymer matrix to produce wider GNRs[25]. At this stage, however, both techniques have limitations. Polymer assisted dispersion has low yields of graphene and few GNRs are found in the suspended material, while the nanotube plasma etching route has limited throughput and scalability. An alternative solution phase chemistry route to GNRs utilizes longitudinal unzipping of carbon nanotubes[26]. Inspired by methods commonly used to oxidize graphite, this approach utilizes potassium permanganate to attack the nanotube sidewalls and sequentially break nearby carbon-carbon bonds. While this technique has the potential to produce large quantities of GNRs, the resulting material is oxidized and thus requires the development of a chemical reduction protocol that regains the properties of pristine graphene.

Progress Towards Monodisperse Graphene Dispersions

To date, most methods of producing monodisperse graphene dispersions have utilized centrifugal processing to remove unwanted graphene or graphitic material. These centrifugal processing techniques rely on the fact that the sedimentation rate of a material is dependent on its shape, size, and buoyant density, as well as the density and viscosity of the centrifugal medium. For instance, to separate graphene by area, a small volume of polydisperse graphene suspension can be placed at the top of a nearly filled centrifuge tube and subject to

high centrifugal forces. In analogy with previous length sorting experiments on carbon nanotubes[27], single-layer graphene flakes with large lateral areas are expected to sediment more rapidly than single-layer graphene with small areas. Consequently, once the centrifugation is complete, the largest graphene flakes, which sediment the furthest, are found near the bottom of the centrifuge tube while the smallest are located near the top.

This type of graphene area sorting has been achieved using nano-GO sheets functionalized with polyethyleneglycol[28]. The functionalized GO was subjected to 2.5 hours of centrifugation at ~300,000 *g* and formed a wide band of material in the centrifuge tube as shown in Fig. 2A. Multiple fractions of sorted GO dispersion were extracted layer by layer and characterized by atomic force microscopy (AFM). Several representative AFM images presented in Fig. 2B-D show a high level of monodispersity in the area of the GO flakes in each fraction with most flakes differing in lateral size by less than 10 nm. As expected, the size of the flakes increased monotonically for fractions extracted progressively closer to the bottom of the tube. In addition, this functionalized GO was found to be biologically compatible and could physisorb high loadings of the anticancer drug doxorubicin, which suggests its use as a drug delivery vehicle.

One of the enabling aspects of the aforementioned lateral area sorting work was the use of GO as opposed to graphene. Since GO is usually dispersed as single layers, the crosstalk between the area and the thickness of the graphene flakes during sedimentation is suppressed. In contrast, a graphene dispersion produced from pristine or expanded graphite generally contains a mixture of different graphene thicknesses and hence a similarly diverse set of buoyant densities. Under some conditions, it is possible to overcome these variations in lateral size and thickness to achieve sedimentation-based sorting. For instance, it has been shown that the proportion of single-layer graphene can be increased in the supernatant after subjecting acetonitrile-graphene dispersions to more aggressive centrifugation conditions.[29] In this case, differences in the graphene buoyant density as a function of layer thickness exceeded the differences established by variations in flake area. For many other situations, however, it is not possible to decouple the effect of area and thickness polydispersity, thus rendering sedimentation-based centrifugal separation ineffective.

In these circumstances, it is possible to use density gradient ultracentrifugation (DGU)[30] to isolate graphene sheets according to their buoyant density. For DGU-based separations, the dispersion of graphene sheets is introduced to a density gradient designed to match the buoyant density distribution of the graphene suspension. Ultracentrifugation of such density gradients causes the graphene sheets to move to their isopycnic points – locations where the density of the medium matches the buoyant density of the graphene. Compared to sedimentation-based separations, DGU-based sorting requires significantly longer centrifugation times since even the slowest moving species must be afforded enough time to reach their isopycnic points. On the other hand, since the buoyant density of a graphene sheet is theoretically independent of lateral area, density gradient processing allows the crosstalk between thickness and area sorting to be minimized for sufficiently long centrifugation times.

Our group has recently succeeded in producing graphene with controlled thickness using DGU[5]. These monodisperse graphene dispersions are generated from aqueous suspensions of graphene encapsulated by the planar surfactant sodium cholate (Fig. 3A), which has previously been used for DGU separations of carbon nanotubes[30]. Ultracentrifugation of sodium cholate dispersed graphene in density gradients results in the appearance of visible bands in the centrifuge tube (Fig. 3B), a characteristic signature of successful isopycnic separations. Extensive AFM measurements following DGU reveal a monotonic increase in the thickness of the graphene with increasing buoyant density (Fig. 3C) and the selective

enrichment of graphene with thicknesses ranging from one to four layers. Using this process, samples with ~85% single-layer graphene have been produced. Furthermore, these results suggest that DGU is an efficient method for generating monodisperse bilayer and trilayer graphene samples that, in contrast to monolayer graphene, are unlikely to be generated preferentially by solution phase exfoliation. Measurements of transparent conductive films generated from DGU-sorted graphene show that predominantly single-layer graphene is approximately three times more conductive than those generated from unsorted graphene produced by weak centrifugation (Fig. 3D). The performance advantage of the sorted graphene material is likely due to its slightly larger lateral areas compared to unsorted graphene, which reduces the number of graphene-graphene contacts required for charge transport, and the improved flexibility of single-layer graphene, which results in more conformal and less resistive junctions between graphene sheets.

Future Outlook

Despite rapid progress in all aspects of solution phase graphene production, a considerable amount of additional work is required before monodisperse “electronics grade” graphene becomes widely available. First, methods of dispersing graphene should be improved to provide higher quality inputs for sorting processes. Liquid phase exfoliation of unfunctionalized graphene sheets greater than ~100 μm^2 in area remains a considerable challenge, although recent experimental results suggest it is possible[31]. Moreover, a scalable method of producing pristine GNRs with sub-10-nm widths and well-defined, precisely oriented, and passivated edges has yet to be developed. Second, new methods of sorting or directly synthesizing monodisperse graphene should be investigated, since it is unlikely that centrifugal processing will efficiently address all sources of graphene polydispersity. Interesting developments in the direct chemical synthesis of graphene via organic[32] and solvothermal[33] techniques may help address this issue. Third, deposition of the output from sorting processes should be improved to facilitate their incorporation into devices ranging from single-layer graphene transistors to graphene-based transparent conductors.

Fortunately, most of the above challenges have already been confronted with carbon nanotubes and can help guide future work. Biomolecules such as DNA[34] and flavin mononucleotide[35] have proven to be exquisitely sensitive to the atomic structure of carbon nanotubes. Similar molecules could be used to exfoliate GNRs with controlled width and edge structure, or facilitate post-dispersion sorting. Furthermore, a variety of sophisticated separation methods have already been developed for carbon nanotubes[36], and based on the success of centrifugal sorting techniques, many of these approaches are likely to be applicable to graphene. Similarly, controlled deposition methods perfected with carbon nanotubes have already been successfully applied to graphene[23,37]. These approaches and others could be used to deposit monodisperse graphene flakes at desired locations or to align sorted GNRs over large areas[38] for a variety of graphene-based applications.

Acknowledgments

This work was supported by the National Science Foundation, Office of Naval Research, Army Research Office, Department of Energy, Nanoelectronics Research Initiative, and National Institutes of Health. A Natural Sciences and Engineering Research Council of Canada Postgraduate Scholarship (A. A. G.) is also acknowledged.

Biographies

Alexander A. Green was born in Ottawa, Canada and received his B.A.Sc. in Engineering Science at the University of Toronto. He is currently pursuing Ph.D. research with Mark C. Hersam at Northwestern University. His research centers on the electronic and optical properties of thin films of monodisperse carbon nanomaterials.

Mark C. Hersam is currently a Professor of Materials Science and Engineering and a Professor of Chemistry at Northwestern University. He earned a B.S. in Electrical Engineering from the University of Illinois at Urbana-Champaign (UIUC) in 1996, M.Phil. in Physics from the University of Cambridge in 1997, and a Ph.D. in Electrical Engineering from UIUC in 2000. His research interests include nanofabrication, scanning probe microscopy, semiconductor surfaces, and carbon nanomaterials. For more information, please visit: http://www.hersam-group.northwestern.edu/.

References

1. Bolotin KI, Sikes KJ, Jiang Z, Klima M, Fudenberg G, Hone J, Kim P, Stormer HL. Ultrahigh electron mobility in suspended graphene. Solid State Commun 2008;146:351–355.
2. Zhang YB, Tan YW, Stormer HL, Kim P. Experimental observation of the quantum hall effect and berry's phase in graphene. Nature 2005;438:201–204. [PubMed: 16281031]
3. Geim AK, Novoselov KS. The rise of graphene. Nature Mater 2007;6:183–191. [PubMed: 17330084]
4. Watcharotone S, Dikin DA, Stankovich S, Piner R, Jung I, Dommett GHB, Evmenenko G, Wu SE, Chen SF, Liu CP, et al. Graphene-silica composite thin films as transparent conductors. Nano Lett 2007;7:1888–1892. [PubMed: 17592880]
5. Green AA, Hersam MC. Solution phase production of graphene with controlled thickness via density differentiation. Nano Lett. 2009 doi: 10.1021/nl902200b.
6. Eda G, Unalan HE, Rupesinghe N, Amaratunga GAJ, Chhowalla M. Field emission from graphene based composite thin films. Appl. Phys. Lett 2008;93:233502.
7. Stankovich S, Dikin DA, Dommett GHB, Kohlhaas KM, Zimney EJ, Stach EA, Piner RD, Nguyen ST, Ruoff RS. Graphene-based composite materials. Nature 2006;442:282–286. [PubMed: 16855586]
8. Novoselov KS, Geim AK, Morozov SV, Jiang D, Zhang Y, Dubonos SV, Grigorieva IV, Firsov AA. Electric field effect in atomically thin carbon films. Science 2004;306:666–669. [PubMed: 15499015]
9. Geim AK. Graphene: Status and prospects. Science 2009;324:1530–1534. [PubMed: 19541989]
10. Park S, Ruoff RS. Chemical methods for the production of graphenes. Nature Nanotech 2009;4:217–224.
11. Zhang YB, Tang TT, Girit C, Hao Z, Martin MC, Zettl A, Crommie MF, Shen YR, Wang F. Direct observation of a widely tunable bandgap in bilayer graphene. Nature 2009;459:820–823. [PubMed: 19516337]
12. Craciun MF, Russo S, Yamamoto M, Oostinga JB, Morpurgo AF, Tarucha S. Trilayer graphene is a semimetal with a gate-tunable band overlap. Nature Nanotech 2009;4:383–388.
13. Neto AHC, Guinea F, Peres NMR, Novoselov KS, Geim AK. The electronic properties of graphene. Reviews of Modern Physics 2009;81:109–162.
14. Son YW, Cohen ML, Louie SG. Energy gaps in graphene nanoribbons. Phys. Rev. Lett 2006;97:216803. [PubMed: 17155765]
15. Han MY, Ozyilmaz B, Zhang YB, Kim P. Energy band-gap engineering of graphene nanoribbons. Phys. Rev. Lett 2007;98:206805. [PubMed: 17677729]
16. Chen ZH, Lin YM, Rooks MJ, Avouris P. Graphene nano-ribbon electronics. Physica E 2007;40:228–232.
17. Niyogi S, Bekyarova E, Itkis ME, McWilliams JL, Hamon MA, Haddon RC. Solution properties of graphite and graphene. J. Am. Chem. Soc 2006;128:7720–7721. [PubMed: 16771469]
18. Hernandez Y, Nicolosi V, Lotya M, Blighe FM, Sun ZY, De S, McGovern IT, Holland B, Byrne M, Gun'ko YK, et al. High-yield production of graphene by liquid-phase exfoliation of graphite. Nature Nanotech 2008;3:563–568.
19. Lotya M, Hernandez Y, King PJ, Smith RJ, Nicolosi V, Karlsson LS, Blighe FM, De S, Wang ZM, McGovern IT, et al. Liquid phase production of graphene by exfoliation of graphite in surfactant/water solutions. J. Am. Chem. Soc 2009;131:3611–3620. [PubMed: 19227978]

20. Stankovich S, Dikin DA, Piner RD, Kohlhaas KA, Kleinhammes A, Jia Y, Wu Y, Nguyen ST, Ruoff RS. Synthesis of graphene-based nanosheets via chemical reduction of exfoliated graphite oxide. Carbon 2007;45:1558–1565.
21. Tung VC, Allen MJ, Yang Y, Kaner RB. High-throughput solution processing of large-scale graphene. Nature Nanotech 2009;4:25–29.
22. Li XL, Wang XR, Zhang L, Lee SW, Dai HJ. Chemically derived, ultrasmooth graphene nanoribbon semiconductors. Science 2008;319:1229–1232. [PubMed: 18218865]
23. Li XL, Zhang GY, Bai XD, Sun XM, Wang XR, Wang E, Dai HJ. Highly conducting graphene sheets and langmuir-blodgett films. Nature Nanotech 2008;3:538–542.
24. Eda G, Chhowalla M. Graphene-based composite thin films for electronics. Nano Lett 2009;9:814–818. [PubMed: 19173637]
25. Jiao LY, Zhang L, Wang XR, Diankov G, Dai HJ. Narrow graphene nanoribbons from carbon nanotubes. Nature 2009;458:877–880. [PubMed: 19370031]
26. Kosynkin DV, Higginbotham AL, Sinitskii A, Lomeda JR, Dimiev A, Price BK, Tour JM. Longitudinal unzipping of carbon nanotubes to form graphene nanoribbons. Nature 2009;458:872–876. [PubMed: 19370030]
27. Sun X, Zaric S, Daranciang D, Welsher K, Lu Y, Li X, Dai H. Optical properties of ultrashort semiconducting single-walled carbon nanotube capsules down to sub-10 nm. J. Am. Chem. Soc 2008;130:6551–6555. [PubMed: 18426207]
28. Sun X, Liu Z, Welsher K, Robinson J, Goodwin A, Zaric S, Dai H. Nano-graphene oxide for cellular imaging and drug delivery. Nano Res 2008;1:203–212. [PubMed: 20216934]
29. Qian W, Hao R, Hou Y, Tian Y, Shen C, Gao H, Liang X. Solvothermal-assisted exfoliation process to produce graphene with high yield and high quality. Nano Res 2009;2:706–712.
30. Green AA, Hersam MC. Ultracentrifugation of single-walled nanotubes. Mater. Today 2007;10:59–60.
31. Tang YB, Lee CS, Chen ZH, Yuan GD, Kang ZH, Luo LB, Song HS, Liu Y, He ZB, Zhang WJ, et al. High-quality graphenes via a facile quenching method for field-effect transistors. Nano Lett 2009;9:1374–1377. [PubMed: 19301858]
32. Yang X, Dou X, Rouhanipour A, Zhi L, Rader HJ, Mullen K. Two-dimensional graphene nanoribbons. J. Am. Chem. Soc 2008;130:4216–4217. [PubMed: 18324813]
33. Choucair M, Thordarson P, Stride JA. Gram-scale production of graphene based on solvothermal synthesis and sonication. Nature Nanotech 2009;4:30–33.
34. Tu XM, Manohar S, Jagota A, Zheng M. DNA sequence motifs for structure-specific recognition and separation of carbon nanotubes. Nature 2009;460:250–253. [PubMed: 19587767]
35. Ju SY, Doll J, Sharma I, Papadimitrakopoulos F. Selection of carbon nanotubes with specific chiralities using helical assemblies of flavin mononucleotide. Nature Nanotech 2008;3:356–362.
36. Hersam MC. Progress towards monodisperse single-walled carbon nanotubes. Nature Nanotech 2008;3:387–394.
37. Vijayaraghavan A, Sciascia C, Dehm S, Lombardo A, Bonetti A, Ferrari AC, Krupke R. Dielectrophoretic assembly of high-density arrays of individual graphene devices for rapid screening. ACS Nano 2009;3:1729–1734.
38. Engel M, Small JP, Steiner M, Freitag M, Green AA, Hersam MC, Avouris P. Thin film nanotube transistors based on self-assembled, aligned, semiconducting carbon nanotube arrays. ACS Nano 2008;2:2445–2452. [PubMed: 19206278]

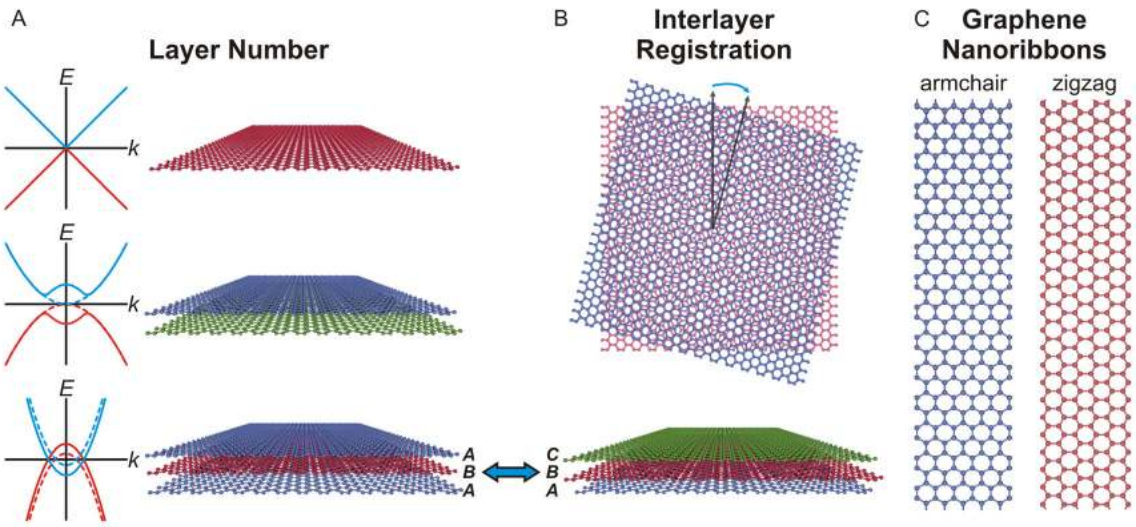

Figure 1.

Polydispersity map of graphene. The electronic and optical properties of graphene depend on (A) layer number and (B) interlayer registration. Schematic band diagrams on the left of panel (A) show graphene band structure with (solid curves) and without (dashed curves) an applied gate bias. (C) Graphene nanoribbons have band gaps that vary as function of their width and edge type.

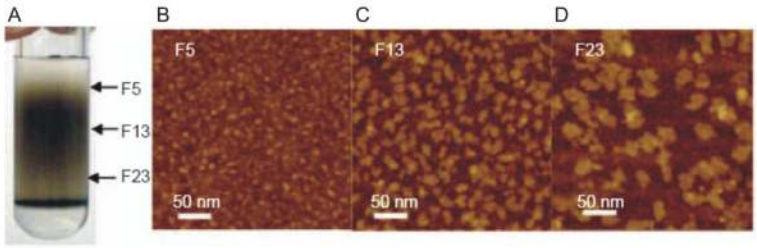

Figure 2.
Area sorting of polyethyleneglycol functionalized graphene oxide (GO). (A) Photograph of the centrifuge tube following ultracentrifugation. (B-D) Representative atomic force microscopy images of the sorted GO taken from the locations marked in panel (A). This figure is adapted from Sun et al.[28]

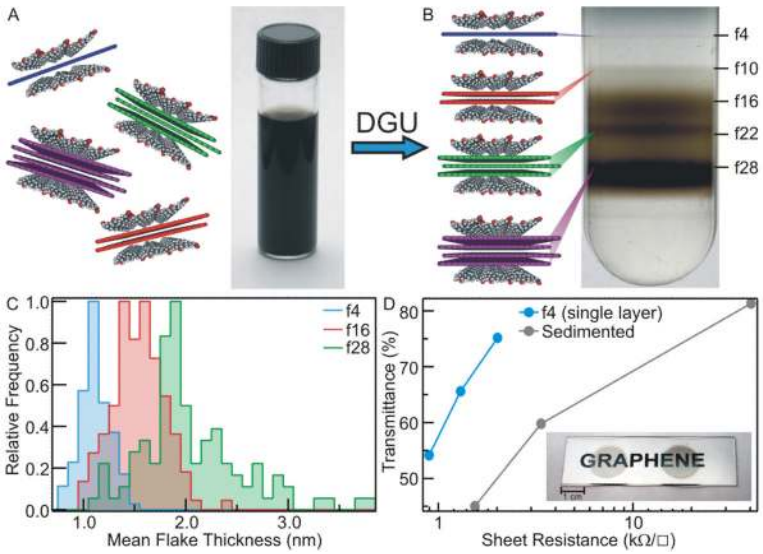

Figure 3.

Thickness sorting of graphene using density gradient ultracentrifugation (DGU). (A) Schematic illustration of ordered sodium cholate encapsulation of graphene sheets and photograph of an unsorted aqueous graphene suspension with a graphene loading of ~0.1 mg mL^{-1}. (B) Photograph of a centrifuge tube following DGU marked with the main bands of monodisperse graphene. (C) Mean flake thickness histogram measured by atomic force microscopy of sorted graphene taken from the locations marked in panel (B). (D) Transparent conductor performance at a wavelength of 550 nm for films made from sorted single-layer graphene (f4) and unsorted (sedimented) graphene. Inset: photograph of sorted graphene transparent conductive films. This figure is adapted from Green and Hersam.[5]